MORPHOLOGICAL PROCESSING OF SEVERELY OCCLUDED DIGITAL ELEVATION IMAGES TO EXTRACT AND CONNECT STREAM CHANNELS

Hyun-chong Cho[1], *K. Clint Slatton*[1, 2]

[1] Department of Electrical and Computer Engineering
[2] Department of Civil and Coastal Engineering
University of Florida; PO Box 116130; Gainesville, FL 32611
Tel: 352.392.0634, Fax: 352.392.0044, E-mail: slatton@ece.ufl.edu

ABSTRACT

Recent advances in technology have enabled the acquisition of high-resolution topographic data by means of Airborne Laser Swath Mapping (ALSM), which can yield Digital Elevation Models (DEMs) with horizontal resolutions of 1m. A DEM is a grayscale image wherein pixel value corresponds to elevation. Using ALSM imaging systems over forested terrain, we filter out the laser returns from the occluding foliage and estimate bare-surface DEMs. Extracting stream networks from DEMs is important for modeling many hydrological processes. We apply a sequence of morphological operations to an ALSM DEM to detect stream channels in forested terrain. We verify the accuracy of the results using a set of error measures over simulated terrain and also using GPS ground truth over real terrain. For linking disconnected stream segments, a measure of pixel connectedness is used.

Index Terms— Lidar, digital elevation models, stream delineation, morphology, connectivity number

1. INTRODUCTION

The accurate delineation of streams is critical to the fundamental understanding of how water flows over terrain, as well as predicting flooding and the transport of pollution. Accurate representation of streams in a Digital Elevation Model (DEM), which is simply an image of topographic elevation, is a required step in simulating and predicting the effects of landscape processes, such as erosion, sediment transport and shallow landslides. The stream network extraction facilitates understanding about how rain water is partitioned into surface runoff and ground infiltration. In turn, it leads to better decision making and planning in water runoff management for sustainable development of water resources [1], [2].

Airborne Laser Swath Mapping (ALSM) systems operate on the lidar, or light detection and ranging, principle. A pulsed laser emits narrow beams of light, while a local clock measures the elapsed time of flight until the reflected photon packet arrives back at the receiver. By knowing precisely the scan angle and aircraft position and orientation, the 3D location of each reflection can be determined. Laser pulse rates of 20 – 50 kHz and side-to-side scan rates of 10 – 40 Hz are common. Therefore, when flying at altitudes of 500m-1000m above the ground, laser beam footprint spacings of 1 point per square meter are typical. The ALSM measurements can be interpolated to generate DEMs with horizontal resolutions of 1m, vertical (elevation) rms errors of 10 – 20 cm, and horizontal rms errors of 20 – 40 cm. Penetration through foliage is achieved via the narrow beam divergence that, for a fraction of the shots, allows much of the pulse energy to reach the ground and return to the receiver.

Previous approaches to stream network delineation were developed using DEMs that have far lower resolution, such as the USGS National Elevation Dataset (NED) [3]. The NED dataset is a seamless DEM of the continental United States derived from stereo aerial photography, acquired over many years, and formatted with 30m horizontal pixel spacing. Thus, previous stream delineation algorithms were developed to infer stream locations from the landform, applying empirical thresholds to ratios of terrain slope and area [4]. Even when high-resolution ALSM elevation images are used, stream networks inferred from DEMs in this manner were found to be significantly different from ground truth in several instances [5]. Thus, there was a need to develop a new method that would explicitly extract stream networks from high-resolution ALSM elevation images.

In this work, we simulate realistic terrain DEMs on which we can calculate several error measures to characterize the performance of our stream detection algorithm. Then we apply the algorithm to actual ALSM data over a challenging test site. The low-relief karst topography of Northern Florida formed in response to erosional processes acting on the carbonate (limestone) bedrock. The drainage of rain water through this landscape has created a complex terrain, known as a multi-basinal drainage pattern that exhibits many small, closed watersheds [6]. Our site consists of an urban forest in the town of

Gainesville, Florida with 30m tall tree canopies dissected by residential streets. The study site was imaged in September 2005 with an ALSM sensor owned by the University of Florida (UF), which is described in [7]. The dense forest cover acts as an occluding medium that dramatically reduces the number of ALSM samples that reach the ground.

2. BASIC ALGORITHM THEORY

Raw ALSM data comes in the form of an irregularly spaced "cloud" of discrete laser returns, and each point is associated with a 3D coordinate. The ALSM point cloud data is first segmented into ground and non-ground points using the method in Kampa and Slatton [8]. The set of ground points is then interpolated to yield a bare-surface DEM. To detect the streams, this input elevation image is smoothed by convolution with a 7×7 diamond-shaped structuring element (SE). Then the inverse tangent is used as a simple non-linear scaling function to emphasize the small variations in elevation between stream channels and the surrounding stream banks.

The bothat morphological operator (inverse of the better known tophat operator) [9] is then applied using the same diamond-shaped SE. The result is an image that displays the stream positions but has a very low contrast. Histogram equalization is performed to further exaggerate the pixel value range. The stream channels are segmented from the surrounding terrain by applying Otsu's method to the grayscale image to form a binary image of stream and "non-stream" pixels [10]. Otsu's method is an unsupervised clustering method that finds the pixel value threshold that maximizes the distance between the two resulting pixel value clusters, normalized by their standard deviations.

The resulting binary image contains the detected streams, but it also contains a small number of short "stray" regions, a common artifact of morphological filters. The "stray" regions are not streams because they do not satisfy the criterion for a minimum length of a stream. These are removed using the simple "area" binary morphological operator that removes connected pixel groups of insufficient area. (110 pixels in this case) To precisely locate the streams, the centerlines are then found using the thinning algorithm in [9]. Overall algorithm details are given in [11].

3. FILTER PARAMETER SELECTION USING SIMULATED TERRAIN

The shape and size of the SE is very important in mathematical morphology. Therefore, after developing the basic algorithm to detect stream centerlines, a sensitivity analysis was performed with respect to the shape and size of the SE. We generate simulated elevation images using a 2D fractal process and embed meandering stream channels of different widths and depths. We then calculate a nominal ALSM scan pattern over this terrain, and randomly remove 80% to 90% of those simulated ALSM points to mimic the occluding effects of a dense forest canopy. The remaining samples represent the ground points and are interpolated to simulate a bare surface DEM obtained from ALSM data.

The stream detection algorithm can make two kinds of errors: false negatives and false positives. A false positive occurs when the algorithm classifies a detected stream centerline pixel as belonging to the stream class but the true stream centerline does not pass through that location. A false negative occurs when the algorithm fails to classify a pixel as "stream" even though the true stream centerline passes through that location (see Fig. 1).

If we let "×"denote a pixel that was detected (classified) as a stream centerline by our algorithm, and "○" denote a pixel that is on the true stream centerline, we can associate each "×" with the nearest "○" (nearest neighbor rule). This establishes a one-way 1-to-1 correspondence between detected stream centerline pixels and true stream centerline pixels. For each of these "×-○" pairs, we compute the Euclidean distance between them in 2D as

$$d_{\times\circ\min} = \sqrt{(\Delta X_{\times\circ\min})^2 + (\Delta Y_{\times\circ\min})^2} \qquad (1)$$

We then label all "×"s outside a search band around the true stream centerline of width 2τ (i.e. $d_{\times\circ\min} > \tau$) as false positives. Based on the known ALSM resolution and nominal stream sizes, we set the width parameter τ of this search band to be 5m.

Let error metric (EM) of the first type EM1 be the total number of false negative pixels, N_{fn}. True stream centerline pixels that have no corresponding detected pixel within the $\pm\tau$ -band are simply summed. There is no distance associated with this error since there is no detected stream centerline pixel in this case. EM2 is the total number of false positives, N_{fp}. These are simply the "×" pixels outside of the search band. No distance is associated with this error since closeness does not count outside the $\pm\tau$ -band.

It is possible to have a false positive inside the $\pm\tau$ -band. However, we will not consider that an error since τ was chosen small to tightly conform to the stream. For those detected points that remain, i.e. "×" pixels that lie inside the $\pm\tau$ -band, we sum their distances to the nearest "○". This gives us $\sum |d_{\times\circ\min}| / N_{\text{TD}}$ for EM3, where N_{TD} is number of true detected pixels. This is simply the mean absolute error. For EM4, we simply sum the three errors, normalized by the number of pixels in the true stream centerline $N_{\circ}$.

$$EM4 = (N_{\text{fn}} / N_o) + (N_{\text{fp}} / N_{\circ}) + (\sum |d_{\times\circ\min}| / N_{\text{TD}}) \qquad (2)$$

In [12], we showed that larger SEs result in more false positives (larger EM2) and are less likely to have stream disconnects (smaller EM1). We tested different SEs by

varying size and shape and found that the 7×7 diamond-shaped SE yields the smallest total error (EM4).

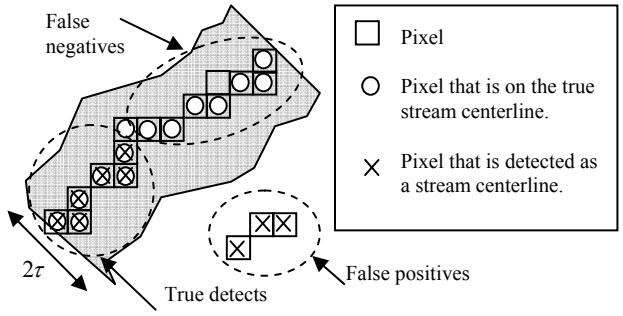

Fig. 1 Definitions of detection errors. The gray area represents a thin band of around the stream center line of width 2τ .

4. CONNECTING STREAM SEGMENTS

As mentioned in Section 1, forest vegetation acts as an occluding medium. Over our test site, it reduced the nominal ground point spacing of 1 point per square meter to roughly 0.12 points per square meter. Because locally dense foliage can preclude ALSM returns from reaching the ground over small areas, it is possible to have some breaks in the detected stream paths. For flow routing however, hydrologists desire unbroken stream paths. Therefore, we must link the stream segments. Several image processing approaches have been developed to link edges or contours in images. In classic edge linking, it is often assumed that two disconnected lines have the same orientation. However, for connecting irregular pixel paths, such as stream centerlines, we require a more general notion of connectedness. We use a connectivity number (CN) [13] to determine when disconnected stream centerlines should be joined.

Given the binary image of detected stream centerline segments and a sliding 3×3 window, the CN specifies the number of black pixels (i.e. value = 1) connected to the center pixel when the center pixel is black (see Table 1). When diagonal connectivity is considered in addition to vertical and horizontal connectivity, it is referred to as 8-connectivity [14]. We have

$$CN^8(x_0) = \sum_{k \in S_1} \left(\overline{f}(x_k) - \overline{f}(x_k)\overline{f}(x_{k+1})\overline{f}(x_{k+2}) \right) \quad (3)$$

where $S_1 = \{1,3,5,7\}$, $\overline{f}(x_k) = 1 - f(x_k)$, and $f(x_k)$ is the value of the k^{th} binary pixel (0 or 1) in the neighborhood. Note the numbering is modulo-8, so that when k =7, we have $x_{k+2} = x_9 = x_1$. CN is a many-to-one mapping that can take on one of five values: CN=0 for an isolated or inner point; CN=1 for an edge point or end point; CN=2 for a connected point; CN=3 for a branch point; and CN=4 for a cross point [14].

Table 1. 3×3 neighborhood for computing 8-connectivity at pixel x_0

$x_4(i-1, j-1)$	$x_3(i-1, j)$	$x_2(i-1, j+1)$
$x_5(i, j-1)$	$x_0(i, j)$	$x_1(i, j+1)$
$x_6(i+1, j-1)$	$x_7(i+1, j)$	$x_8(i+1, j+1)$

End points (CN=1) are candidates for joining, but before connecting the main stream segments, small stream branches must be removed to prevent erroneous connections in this complex multi-basinal area. These are removed using the distance between end points (CN=1) and branch points (CN=3). Wherever that distance is less than 10 pixels, the branch is removed.

There are two criteria for the connecting process, one based on distance and another on pixel value difference in the original grayscale DEM image. The distances between all end points are calculated. Each end point is associated with its nearest neighbor end point. If the distance between those neighbors is smaller than a user defined bound (15 pixels in this case), they become a candidate pair for linking. The distances are then normalized to vary from 0 (farthest) to 1 (closest). For the difference criterion, the average pixel value under a 3×3 window centered at each candidate end point is calculated. For each end point candidate pair, the difference between these two average values is calculated and normalized to vary from 0 (biggest) to 1 (smallest). Elevation difference is used as a criterion to avoid linking meandering stream segments that might be close in horizontal distance, but not in distance along the stream.

Using these distance and difference criteria, we form a simple decision rule using a decision value (DV) and a weight parameter α as in (4). Since the disconnected stream end points tend to be close together, we give greater weight to the distance criterion, so that α = 0.8. Each candidate group thus is labeled with a decision value from 0 (no need to connect) to 1 (should connect). When DV>0.25, the candidate end point pair is connected by a straight line.

$$DV = \alpha \cdot \text{Distance} + (1-\alpha) \cdot \text{Difference} \quad (4)$$

5. RESULTS AND DISCUSSION

The result of applying the segmentation to a heavily forested test site is shown in Fig. 2. The site is an urban forested floodplain. The forest is composed of mixed hardwood and pine trees with dense understory vegetation that completely obscures the streams from traditional aerial photography. The detected stream centerlines were verified using GPS survey points taken in the stream centers.

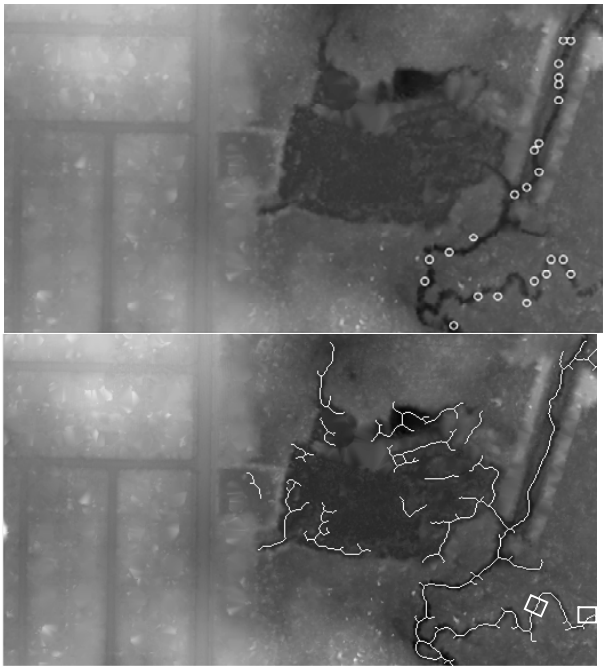

Fig. 2 (Top) 1m×1m bare-surface DEM of an urban forest test site. The 300m×600m surface is largely occluded by 30m tall forest canopy and presents a complex stream network with confluences and ponds. Relative elevations range from 0m (dark) to 5.5m (light). GPS survey points are indicated with circles. (Bottom) Extracted stream centerlines overlaid on the DEM. White boxes indicate locations where particularly dense canopy precluded the detection of the stream channel, thus necessitating the segment connection step.

An Ashtech Z-extreme GPS receiver was run at a solution rate of 1 Hz. Due to the severe canopy attenuation and multipath, the nearly 25 GPS survey locations were occupied for almost one minute each to achieve a GPS horizontal rms position error of 0.72 m (excluding locations where solutions were too sparse for a reliable position estimate). This error was estimated from the average standard deviations in X and Y solutions from the GPS survey points as $\sqrt{\bar{\sigma}_X^2 + \bar{\sigma}_Y^2}$. The orthogonal distance from the nearest detected stream centerline pixel to each GPS point was then computed for the detection error. The minimum, maximum, mean, and standard deviation of the error were 0m, 8.94m, 3.43m, and 2.56m, respectively. The mean error is quite small considering the nominal GPS error for measurements taken under dense canopy.

Stream channel delineation is a very useful operation that leads to better decision making and planning for water resource managers. The growing use of ALSM DEMs in watershed analysis necessitates the modernization of stream detection algorithms that fully exploit high resolution ALSM elevation images. Once the stream pixels are extracted, it is then possible to compute many parameters of import to hydrologists, such as channel width and bank height along the streams.

Results over simulated and actual ALSM DEMs indicate that our approach performs well at detecting small and complex stream channels, even under dense forest canopies. Future work will focus on optimizing the selection of the weight α and DV threshold.

6. ACKNOWLEDGMENTS

This work was supported in part by the NSF National Center for Airborne Laser Mapping (NCALM). The authors wish to thank Ms. Pravesh Kumari for processing the GPS data.

7. REFERENCES

[1] SG Walesh, *Urban Surface Water Management* , Wiley-IEEE, 1989, ISBN: 0471837199

[2] Knighton, D., *Fluvial Forms and Processes: A New Perspective*, Wiley & Sons, New York, NY, 1998, ISBN 0-470-25556-0

[3] USGS NED dataset, http://seamless.usgs.gov/

[4]ESRI,http://www.esri.com/news/releases/02_3qtr/archydro.html

[5] J. P. Walker, G. R. Willgoose. *On the effect of digital elevation model accuracy on hydrology and geomorphology,* Water Resources Research,vol. 35, July 1999

[6] Ritter, D. F., *Process Geomorphology*, WM.C. Brown, Dubuque, Iowa, 1978. ISBN 0-697-05035-1.

[7] Slatton, K. C., W. Carter, and R. Shrestha, "A Simulator for Airborne Laser Swath Mapping via Photon Counting," *Proc. SPIE 2005 Defense and Security Symposium*, vol. 5794, Mar. 2005, pp. 12-20.

[8] Kampa, K. and K. C. Slatton, "An Adaptive Multiscale Filter for Segmenting Vegetation in ALSM Data," *Proc. IEEE 2004 International Geoscience and Remote Sensing Symposium (IGARSS)*, vol. 6, Sep. 2004, pp. 3837 - 3840.

[9] Gonzalez, R. C. and R. E. Woods, *Digital Image Processing*, 2nd ed., Prentice Hall, 2002.

[10] Otsu, N., "A Threshold Selection Method from Gray-Level Histograms," *IEEE Transactions on Systems, Man, and Cybernetics*, Vol. 9, No. 1, 1979, pp. 62-66.

[11] H. Cho, S. Srinivasan, A. Sedighi, K. C. Slatton, "Extraction of Stream Channels in High-Resolution Digital Terrain Images Using Morphology," *Proc. IEEE International Geoscience and Remote Sensing Symposium (IGARSS)*, 2006, pp. 1078 – 1081.

[12] Hyun-chong Cho, Kittipat Kampa, and K. Clint Slatton, "Morphological Segmentation of Lidar Digital Elevation Models to Extract Stream Channels in Forested Terrain," *Proc. IEEE International Geoscience and Remote Sensing Symposium (IGARSS)*, 2007, in press.

[13] Japan Industry Technology Center, *Introduction of Computer Image Processing (Korean version)*, Mechanics Research Press, Seoul, 1993.

[14] W. Zhang, and S. Wang, "An Efficient Connectivity-Number-Based Edge Detection Method for Binary Images," *IEEE Proceeding of the International Conference on Machine Learning and Cybernetics*, vol. 9, 2005, pp. 5324 – 5329.